Indian Journal of Chemical Technology
Vol. 24, September 2017, pp. 498-507

Synthesis and characterization of β-cyclodextrin coated Fe_3O_4/carbon nanocomposite for adsorption of tea catechin from aqueous solutions

Aniruddha Gogoi[1], Madhukar Navgire[2], Kanak Chandra Sarma[1] & Parikshit Gogoi*[,3]

[1]Department of Instrumentation & USIC, Gauhati University,Guwahati 781 014, Assam, India

[2]Department of Chemistry, Jijamata College of Science & Arts, Bhende, Ahmadnagar, Maharastra, India

[3] Department of Chemistry, Nowgong College, Nagaon 782 001, Assam, India

E-mail: parikk100@gmail.com

Received 7 May 2016; accepted 10 December 2016

β-cyclodextrin (β-CD) coated Fe_3O_4/carbon nanocomposite materials have been prepared by co-precipitation and impregnation method for adsorption of tea catechin from aqueous solutions. The prepared catalysts have been characterized by X-ray diffraction, FT-IR spectrometer, SEM, TEM, TGA, Pyridine FTIR and VSM analysis. The particle diameter and saturation magnetization value of Fe_3O_4/carbon is found to be 25-50 nm from TEM analysis and 4.4 emu/g from VSM analysis and decreases after coating of β-CD on Fe_3O_4/carbon nanocomposite to 20-35 nm and 1.2 emu/g, respectively. The adsorption behaviors of tea catechin on β-CD coated Fe_3O_4/carbon nanocomposites have been investigated schematically. The experimental adsorption affinity is interpreted with the help of Langmuir and Freundlich adsorption isotherms and the Langmuir model is found to be best suitable for the experimental data. The adsorption reaches the equilibrium within 90 min. and follows 1st order kinetics. The adsorption process depends on temperature, *p*H and amount of adsorbate and adsorbent.

Keywords: β-CD, Fe_3O_4/carbon nanocomposites, Tea catechin, Freundlich isotherm, Langmuir isotherm

Catechins, a class of flavonoids found in green tea and has been of great interest due to its diverse nutraceutical properties, such as antioxidant, anti-obesity, hypolipidemic and anticarcinogenic activities[1-3]. Currently, intensive research is going on analytical and preparative scale separation methods of tea catechins from its sources which depend on the activity and stability at different media after separation and the viability of scaling up the process[4-7]. Different analytical methods like reversed-phase high performance liquid chromatography (HPLC), normal-phase HPLC-MS, capillary electrophoresis, micellar electro kinetic chromatography and ion exchange chromatography have been used for the separation and characterization of tea polyphenols[8-10]. In general, the extraction and purification of tea catechins have been done by conventional solvent extraction, membrane based separation, supercritical fluid extraction and adsorptive separations by using activated carbon and polymeric resins[11-18]. Among these methods, adsorption using magnetic nanocomposite materials have been increasingly received attention due to its advantageous properties like extremely small size, good dispersibility in various solvents, high surface area, magnetic responsivity and the absence of internal diffusion resistance which provides better kinetics for adsorption of solutes from aqueous solution[19]. Moreover, magnetic nano-adsorbents can be recovered from the solution phase with an external magnetic field. The incorporation of magnetic particles with other functionalized materials like multi-walled carbon nanotubes, activated carbon etc., which are effectively used for removal of both organic and inorganic molecules from aqueous solutions makes it more attractive due to easy separation and recovery of the adsorbents[20-22]. The surfaces of these particles are further modified by natural or synthetic polymers such as chitosan, gum arabic, alginate, poly (acrylic acid), β-CD, dextran etc. to make them more stable, biocompatible, and suitable for applications as adsorbents[23-27]. However, the effectiveness of magnetic Fe_3O_4/carbon nano-adsorbents coated with β-CD has not been reported in literature for adsorptive separation of tea catechins from aqueous solutions.

Cyclodextrins (CDs) are a class of natural cyclic oligosaccharides having six, seven, or eight glucose

subunits linked by α-(1, 4) glycosidic bonds with a torus shaped structure and are classified as α-, β-, and γ-CD respectively. The structure of cyclodextrin molecules containing a polar cavity with primary hydroxyl groups lying on the outside and the secondary hydroxyl groups inside[24,25]. The special arrangement of hydroxyl groups in CDs permits a variety of organic and inorganic compounds to form inclusion complexes in its hydrophobic cavity which makes it promising for applications in drug delivery systems, nanoreactors, bioactive supramolecular assemblies, molecular recognition, and catalysis. However, these powdery cyclodextrin-based adsorbents are very difficult to separate from solutions except high speed centrifugation which limits their practical applications. The combination of CDs and magnetic nanoparticles provides an alternative method to separate powdery adsorbents from solution effectively[23,27].

In view of the importance of this research area, we report here the preparation and characterization of Fe_3O_4, Fe_3O_4/carbon and β-CD coated Fe_3O_4/carbon nanocomposites for the adsorption of (+)-catechin from aqueous solutions. The adsorption capacities of the prepared nanocomposites were analyzed at 25°C and experimental equilibrium data were fitted to Langmuir and Freundlich isotherm models. The Van't Hoff plot was used to estimate the heat of adsorption by performing the adsorption experiments at different temperatures.

Experimental Section

Materials

The chemicals used for this study, namely (+)-catechin (C), $FeCl_2.4H_2O$, $FeCl_3.6H_2O$ and β-cyclodextrin were obtained from Sigma Chemical Co., USA. The buffer solutions prepared from potassium dihydrogen phosphate and dipotassium hydrogen phosphate were supplied by Qualigens, India; ammonia solution was purchased from Merck, India. All the chemicals were of analytical grade and used without further purification. Double distilled deionised water was used for the adsorption studies. The carbon used for the preparation of composite was synthesized from *Acacia arabica*plant (wild Babul) as a natural source. The dried wood was burnt in the absence of air and the resulting charcoal was crushed into fine powder. The finely grounded powder material was calcined at 500°C for 3 h. in a high temperature muffle furnace in air atmosphere. The temperature stability of carbon is estimated to be up to 2800°C in vacuum and about 750°C in air[28].

Methods

Preparation of Fe_3O_4/carbon

Fe_3O_4/carbon nanocomposite was prepared by conventional standard impregnation method. To impregnate carbon-doped Fe_3O_4, the solution was obtained by dissolving required amount of $FeCl_2.4H_2O$ and $FeCl_3.6H_2O$ in deionized water separately, mixed together under vigorously stirred condition and stirring continued until a clear solution obtained. The mixed solution was precipitated by drop-wise addition of aqueous ammonia solution (1:1) until the solution *p*H reached ~8.5. The finely powdered carbon was then added to the solution and stirred contentiously for 2 h. The resulting black coloured slurry was decanted, filtered and washed several times with double distilled water until free from anion impurities. The obtained precipitate was oven dried at 90°C for 12 h. and 500°C for 2 h. in air atmosphere.

Preparation of β-CD coated Fe_3O_4/carbon nanoparticles

Prepared Fe_3O_4/carbon nanoparticleswere mixed with distilled water to make a colloidal solution. The colloidal solution was mixed with β-CD (1wt. % of catalyst) under intense stirring at 40°C. The formed nanoparticles were collected by filtration. The particles were washed with distilled water repeatedly and dried for 24 h. in oven at 90°C.

Instrumental measurements

The crystalline nature of the synthesized samples were investigated by X-ray diffraction (XRD) pattern recorded on a Bruker (D2 phaser) using Cu-K_α radiation (λ= 1.514Å). The FT-IR studies were recorded using a Perkin-Elmer (Spectrum Two) FT-IR spectrometer in KBr pellets. The surface morphology of the samples was carried out using scanning electron microscopy (SEM) characterization conducted using a Jeol-JED 2300 (*L*A) instrument. Thermogravimetric analysis (TGA) was investigated by Mattler Toledo (TGA/SDTA 581) thermogravimetri canalyzer over a temperature range of 30–700°C with a heating rate of 10°C min^{-1} under nitrogen atmosphere. The microscopic nanostructure and particle size was determined using a CM-200 Philips TEM at 200 kV (L = 600, l = 0.0025 nm). The magnetic properties recorded for the samples using a vibrating sample magnetometer (Lakeshore 7410) and spectrophotometric study were recorded on a UV- vis spectrophotometer (Shimadzu/ UV- 1800).

Adsorption experiments

The adsorption equilibrium studies for the (+)-catechinwas obtained at *p*H 7. The *p*H of solutions were maintained at 7 by using phosphate buffer reagents of appropriate dosages and measured with a pH meter. The initial catechins concentrations were taken between 5 and 10 mM at 25±0.5°C for 3-4 h. to obtain the linearity in the adsorption isotherm. The adsorption equilibrium was achieved within 90 min. of contact time for all tested catalyst as confirmed by preliminary runs of the experiments. After the equilibrium was reached, the aqueous phase was analyzed by a UV-Vis spectrophotometer for solute concentrations. The calibration curve of (+)-catechin was made by measuring absorbance at λ_{max} 280 nm for the determination of concentrations. The reproducibility of UV-Vis analysis was found to be ± 2% and the experiments were carried out in duplicate. The adsorption enthalpies were estimated from adsorption affinity by conducting equilibrium experiments at two other temperatures 45°C and 60°C. The adsorbents used were Fe_3O_4, Fe_3O_4/carbon and β-CD coated Fe_3O_4/carbon nanocomposite materials. The amounts of catechins adsorbed per gram of adsorbent q (mmol/g) were calculated from the following equation

$$q = V(C-C_e)/W \quad ...(1)$$

where, C and C_e are the initial and equilibrium solute concentrations (mmol/l), V is the solution volume (l) and W is the weight of the adsorbent (g). All the experiments were performed in triplicate and the reproducibility was found to be ± 2%. The adsorption affinity (q/C_e) can be determined numerically by two techniques; (1) averaging the individual values of q/C_e and (2) evaluating slope of the best-fit line for the isotherms. Low concentrations of catechin were used in adsorption equilibrium studies to limit the adsorption to the linear region of the isotherm and all the isotherms could be extrapolated to the origin. The experimental adsorption affinities (q/Ce) were calculated from the slopes of individual isotherms in the linear region and which are identical to the averaged values of individual adsorption affinities of catechins.

Results and Discussion

Magnetic properties analysis

To determine the magnetic properties of obtained Fe_3O_4/Carbon and β-CD coated Fe_3O_4/carbon nanocomposites, the magnetic-hysteresis (MH) loops of the samples were recorded at room temperature and the results were presented in Fig. 1(a). It can be seen that both Fe_3O_4/carbon and β-CD coated Fe_3O_4/carbon nanoparticles exhibit hysteresis which confirms the typical ferromagnetic behavior of the nanoparticles

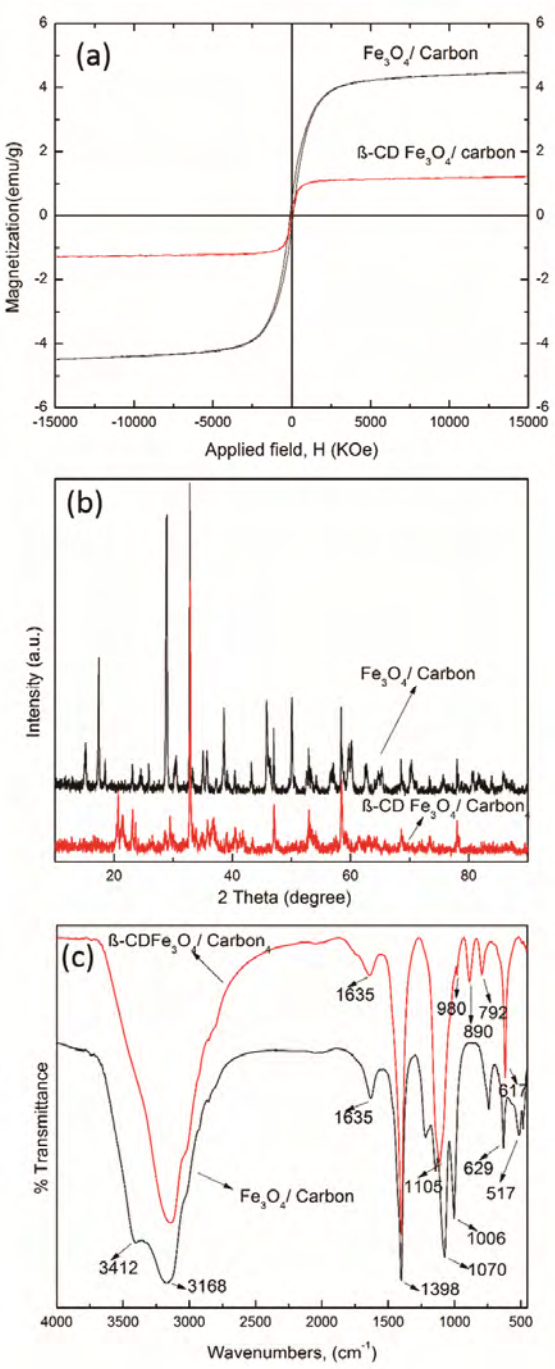

Fig. 1 — Magnetic hysteresis of Fe_3O_4/carbon and β-CD coated Fe_3O_4/carbon magnetic nanocomposites (a); XRD spectrum of Fe_3O_4/carbon and β-CD coated Fe_3O_4/carbon (b); and FT-IR spectrum of Fe_3O_4/carbon and β-CD coated Fe_3O_4/carbon (c).

with negligible coercivities and moderate saturation magnetizations. From MH loops, the saturation magnetization value (*M*s) of Fe_3O_4/carbon and β-CD-Fe_3O_4/carbon were found to be 4.4 emu/g and 1.2 emu/g, respectively. Since the composites were mixed with two non-magnetic materials viz. carbon and β-CD, so for β-CD coated Fe_3O_4/carbon, the magnetization obtained at same field was lower than that of Fe_3O_4/carbon nanoparticles. This is mainly due to the presence of non-magnetic (β-CD layer) on the surface of Fe_3O_4/carbon nanoparticles which act as an electromagnetic shield, consequently yields in a low saturation magnetization. The results are found to be in conformity with the results reported for the β-CD modified hybrid magnetic nanoparticles of Fe_3O_4@SiO_2-PGMACD in literature for which the saturation magnetization was found to be 5.50 emu/g[29].

XRD analysis

Structural and crystalline phase of the magnetite nanocomposites was confirmed by XRD. Figure 1(b) shows the XRD patterns of the nanocomposites. For Fe_3O_4/carbon diffraction peaks were observed at 2θ° = 32.8, 35.7, 43.2, 53.0, 57.2 and 62.8; these peaks can be readily indexed to (220), (311), (400), (422), (511) and (440) reflection planes of cubic Fe_3O_4 and these results were consistent well with the standard diffraction data for Fe_3O_4 (JCPDS Card No.:19-0629). Similarly, for pure carbon highly intense peaks observed at 2θ° = 23.0, 25·98, 28.98, 38·50, 45·7, 50.0, 60.3, 68.4, and 78.25 can be indexed to (321), (400), (124), (600), (345), (137), (760), (210), and (882) planes, which predict the cubic crystal symmetry of carbon substrate or fullerene. It was found that all XRD reflections of carbon substrate were matched using JCPDS card No. 79-1715. For β-CD coated Fe_3O_4/carbon similar pattern were observed with a slight shifting of some peaks and missing/appearance of new peaks were due to the coating of β-CD on the composite. The moderate sharp and distinct peaks suggest that Fe_3O_4 and β-CD coated Fe_3O_4/carbon nanocomposites were highly crystalline. It was also observed that in the present method crystallinity and phase of Fe_3O_4/carbon nanoparticles do not much affect even after coating with β-CD.

The average crystal size (D) of Fe_3O_4/carbon and β-CD coated Fe_3O_4/carbon nanocomposites were determined by using following Scherrer's equation[30]

$$D=(0.9\lambda)/\beta\cos(\theta) \quad ...(2)$$

where, λ is the wave length of CuKα radiation (0.1514 nm), β is the Full Width at Half Maximum (FWHM in radian) of most intense diffraction peak i.e., (311) and (124) reflection peak and θ is the corresponding diffraction angle. In the present case, mean crystallite size of the Fe_3O_4/Carbon and β-CD coated Fe_3O_4/carbon nanocomposites were found to be 33.31 and 24.65 nm respectively shown in Table 1.

FT-IR analysis

The FT-IR spectroscopy was used to confirm the binding of β-CD on the surface of Fe_3O_4/carbon nanocomposites. Figure 1(c) shows FT-IR spectra of Fe_3O_4/carbon and β-CD coated Fe_3O_4/carbon. The absorption band appeared at 629 and 517 cm^{-1} in the Fe_3O_4/carbon spectra assigned to characteristic vibration of Fe-O bonds in the tetrahedral sites of magnetite nanoparticles. For carbon characteristic peaks appeared at 1398 cm^{-1} for aromatic C=C stretching mode, peak at 1006 cm^{-1} is primarily due to C-R stretching frequency. The broad absorption band present in the spectra at around 3150 cm^{-1} can be assigned to the -OH stretching vibration originating from surface hydroxyl groups on the nanocomposites. The above characteristic bands were observed with a little shift in the β-CD coated Fe_3O_4/carbon spectra after modification with β-CD. In these spectra the peaks in the range of 1200 to 900 cm^{-1} are the characteristic peak of β-CD. In addition, the absorption band 1635 cm^{-1} refers to the remaining water.

SEM studies

Figure 2(a and b) shows SEM morphology images of prepared nanocomposites. It shows mesoporous crystal structure for the pure cubic type of modified magnetite Fe_3O_4 nanocomposite material. Figure 2(a) shows morphology of Fe_3O_4/carbon, which shows highly crystalline structure. Further, the addition of β-CD to the Fe_3O_4/carbon, the decreased in the crystallite size was observed, which was clearly seen in

Table 1— Crystallite size calculated using Debye–Scherrer formula

Entry	Catalyst	2θ°	hkl	FWHM	Size (nm)
1	Fe_3O_4/carbon	35.7	311	0.2467	33.31
2	β-CD coated Fe_3O_4/carbon	28.98	124	0.3071	24.65

Fig. 2(b). So, from the SEM micrograph the effect of addition of β-CD can be seen, which clearly shows the alteration in crystallite size and improvement in morphology.

TEM analysis

It is clearly seen from the TEM images that the synthesized material with nano-sized particles have clarity. The TEM image of Fe_3O_4/carbon in Fig. 2(c) shows the presence of mesoporus nature with particle size varying in between 25 nm and 50 nm. While the TEM image of modified Fe_3O_4/carbon with β-CD (Fig. 2d) shows the presence of highly mesoporous material with decrease in particle size between 20 nm and 35 nm. This decrease in size is mainly due to addition of β-CD.

TG analysis

To understand the change in weight percent with respect to change in temperature, thermogravimetric analysis (TGA) was performed on Fe_3O_4/carbon and β-CD coated Fe_3O_4/ carbon samples. Figure 3(a) shows the TGA results plotted in the temperature range of 30°C to 700°C. β-CD coated Fe_3O_4/ carbon sample shows higher weight loss (7% more) as compared to Fe_3O_4/carbon, since β-CD has changed the thermal degradation properties of β-CD coated Fe_3O_4/carbon. Its first weight loss in 30-70°C regions corresponds to the loss of water molecule and the second degradation starts around 170°C. The first weight loss for the Fe_3O_4/carbon is not significant and its degradation starts at around 170°C. In addition, the decomposition for β-CD at around 290°C was observed in β-CD coated Fe_3O_4/carbon.

The second weight loss took place between 380-480°C for both the samples were due to loss of ammonia compounds. Another weight loss at 570-640°C could be responsible for dehydration of hydroxyl groups. However, in the temperature above 650°C both the samples were quite thermally stable and indicates the achievement of thermally stable catalyst.

Pyridine FTIR spectroscopy study

To understand the Bronsted and Lewis acid sites in the samples, Pyridine FTIR spectroscopy was performed in the range of 1900–1400 cm^{-1}. Figure 3(b) shows the Pyridine FTIR spectroscopy of Fe_3O_4/carbon and β-CD coated Fe_3O_4/carbon samples. It is observed that both the samples exhibited prominent peaks in the range of 1700-1400 cm^{-1}.The peak around 1639 cm^{-1} can be assigned as the pyridine adsorbed on Bronsted acidic sites whereas

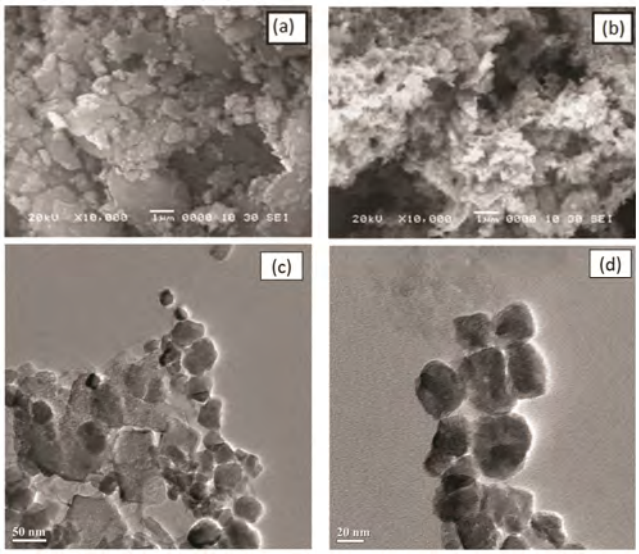

Fig. 2 — SEM images of Fe_3O_4/carbon (a) and β-CD coated Fe_3O_4/carbon (b); TEM images of Fe_3O_4/carbon (a) and β-CD coated Fe_3O_4/carbon (b).

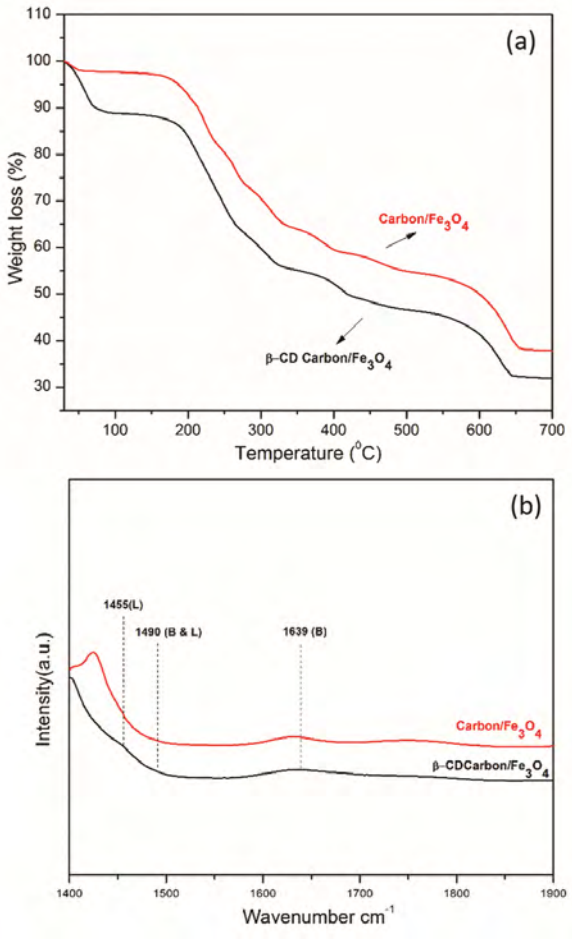

Fig. 3 — TGA graphs of Fe_3O_4/carbon (a) and β-CD coated Fe_3O_4/carbon (b); Pyridine FTIR spectrum of Fe_3O_4/carbon (a) and β-CD coated Fe_3O_4/carbon (b).

peak at 1455 cm^{-1} can be assigned as the pyridine adsorbed on Lewis acidic sites. There is also a broad IR band at 1490 cm^{-1}, which is the indication of the presence of both Bronsted and Lewis acidic sites[31]. The Bronsted acidic sites present in the catalyst played an important role in the oxidation reaction at room temperature.

Adsorption equilibrium

Adsorption isotherms measured for (+)-catechin on Fe_3O_4, Fe_3O_4/carbon and β-CD coated Fe_3O_4/carbon nanocomposites are shown in Fig. 4(a). The adsorption isotherm of (+)-catechin was obtained in different concentration range of liquid phase as with the adsorbents, due to different adsorption capacity of adsorbents. The experimental data of Fig. 4(a) shows that β-CD coated Fe_3O_4/carbon nanocomposite has greater q values than the other adsorbents at all aqueous (+)-catechin concentrations and may be considered as the most appropriate for removing the (+)-catechin from aqueous solutions. The adsorption of catechin on different polymeric resins, activated carbon and metal oxides are complex and mechanisms are driven by various attractive forces.

The effect of *p*H on (+)-catechin adsorption on β-CD coated Fe_3O_4/carbon nanocomposite is shown in Fig. 4(b). The variation of *p*H is marginal due to the polar-polar interactions with the acid nature of (+)-catechin with the β-CD on the Fe_3O_4. At *p*H 7 the observed value of q was maximum so all other experiments for this study were carried out at *p*H 7.

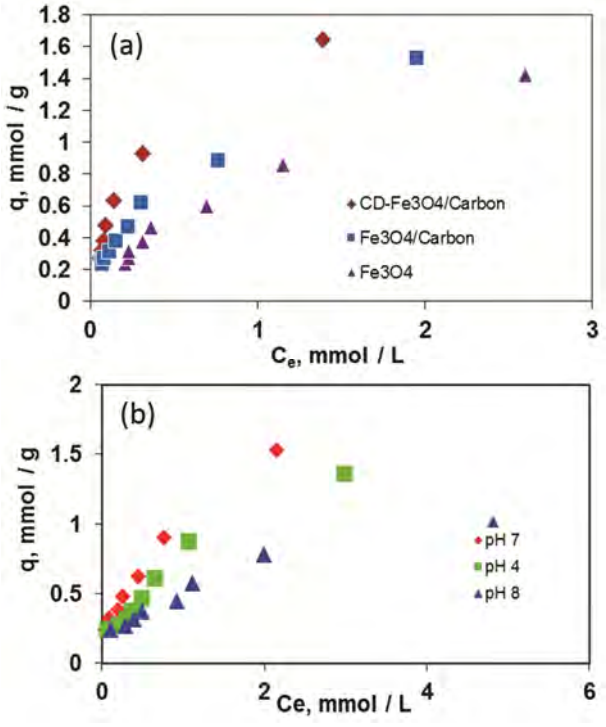

Fig. 4 — Adsorption isotherm of (+)-catechin on different adsorbents (a) and effect of pH on the adsorption of catechin onto β-CD coated Fe_3O_4/carbon (b).

Phenolic compounds are adsorbed by activated carbon**,** which interacts through hydrogen bonding due to the presence of carbonyl, carboxyl, phenolic hydroxyl, lactone and quinine groups at the surface. An adsorption process is governed by different external physicochemical parameters such as *p*H, temperature, competing compounds present in solution, the chemical structure of adsorbents or other characteristics such as particle size, porosity, adsorbent polarity, specific surface area, and pore volume distribution[31,32]. In the present study chemical nature of the adsorbents play more dominant rule than the physical structure on (+)-catechin adsorption. β-CD coated Fe_3O_4/carbon nanocomposites, which gives the best result in terms of the adsorptive capacity, is a magnetic material consisting of polar -OH groups of β-CD and polar groups of activated carbon with a cage like structure, which makes the catalyst more efficient for adsorption of compounds of lower hydrophobicity. Fe_3O_4 and Fe_3O_4/carbon, which are also magnetic material, shows intermediate capacity for the adsorbates due to their more hydrobhobic nature. So, the observed trends of adsorption affinity of (+)-catechin for β-CD coated Fe_3O_4/carbon nanocomposite may be due to the hydrophilic nature of (+)-catechin which are in accordance with the results reported in literature for adsorption of polyphenols on macroporous resins[34]. The adsorption mechanism can be predicted from the experimental values of adsorption intensity. The adsorption of phenol from non-aqueous solutions on activated carbon, acrylic ester polymer and amide containing resins are driven by hydrogen bonding mechanism whereas hydrophobic interaction is dominant over hydrogen bonding from aqueous solutions since hydrogen bonding alone in aqueous solution is very weak because of the strong hydrogen bonding characteristics of water[35,36].

Adsorption isotherm

The Langmuir and Freundlich isotherm models were used to interpret the adsorption equilibrium. The values of isotherm parameters estimated by non-linear regression analysis are shown in Table 2. The Langmuir model provides identical fit of experimental data at almost for all the nanomaterials studied. Table

Table 2 — Parameter values for the adsorption of (+)- catechin at 25°C

Adsorbent	Langmuir $q=KX_m / (1+KC_e)$			Freundlich $q=K_FC_e^n$		
	K	X_m	R^2	K_F	n	R^2
β-CD coated Fe_3O_4/carbon	1.2154	1.7289	0.9856	1.1134	0.6845	0.9856
Fe_3O_4/carbon	0.0429	1.3455	0.9851	0.3754	0.5428	0.9850
Fe_3O_4	0.0127	1.0124	0.6821	0.1194	0.4429	0.7745

2 shows the value of the isotherm parameters estimated by non-linear regression analysis. Comparing the coefficients of determination (R^2) of the models it appears that Langmuir isotherm provides the most satisfactory representation of the experimental data almost at all experimental sets. The adsorption of phenols, flavonoids, tea catechins on different resins, activated carbon and lignocelluloses can be interpreted satisfactorily with the help of Langmuir, Freundlich and Redlich-Peterson isotherm models[32,34-37].

The nature of the solute-surface interaction can be interpreted from the isotherm of adsorption of solute from aqueous solutions. In this study, we have estimated theLangmuir class of adsorptionisotherm with a linear initial part showing the high diffusion of solute into the adsorbent which implies no strong competition between solute and solvent. Liquid phase concentration C_{ref} Langmuir analysis[38] was established to describe the type of isotherm for a given equilibrium. The relationship used was originally described by Vermeulan*et al*.[39] as

$$\bar{r} = \frac{1}{1+ KL\ C_{ref}} \qquad ...(3)$$

The value of $\bar{r}$ determines the type of isotherm follows as listed in Table. 2

$0<\bar{r}<1$ ------ favourable

$\bar{r}>1$ ------ unfavourable

$\bar{r}=1$ ------ linear

$\bar{r}=0$ ------ irreversible

The calculated values of the constant $\bar{r}$ were in the range of 0.01967 to 0.32256 for the tested magnetic adsorbents. These values of Langmuir constants are marginally higher than those for adsorption of total phenolics and total flavanoidson polymeric resins[34,35].

Adsorption enthalpy

The adsorption enthalpy can be calculated by using temperature dependence of adsorption affinity q/C_e (where C_e is equilibrium solute concentration) using Van't Hoff's thermodynamic relationship:

$$\Delta G^0 = - RT \ln K = - RT \ln\{\Psi (q / C_e)\} \qquad ...(4)$$

where, ΔG^0 is the standard free energy of adsorption, R is the universal gas constant, T is the temperature in Kelvin, K is the equilibrium constant for the adsorption process and Ψ is a proportionality constant which includes terms for the activity coefficients of the solute in the two phases and the activity of the unbound adsorption sites. By keeping low solute concentration, adsorption was limited to the linear region of the isotherm; the equilibrium constant can be directly related to the adsorption affinity[40]. As we consider a narrow range of solute concentrations (in both the solid and liquid phases), it is possible that Ψ will be constant over the condition applied.

The second thermodynamic relationship used in the Van't Hoff method is:

$$\Delta G^0 = \Delta H^0 - T\Delta S^0 \qquad ...(5)$$

where, ΔH^0 and ΔS^0 are the standard enthalpy and entropy changes of adsorption, respectively. Combining Eqs. (4) and (5), we have:

$$\ln (q / C_e) = - \Delta H^0 / RT + [\Delta S^0 / R - \ln \Psi] \qquad ...(6)$$

If ΔH^0, ΔS^0 and Ψ remain constant over the temperature range studied, a plot of ln(q/Ce) versus 1/T yields a straight line with a slope of $-\Delta H^0 /R$, from which ΔH^0 can be calculated.

The effect of temperature on the adsorption equilibrium was evaluated by performing the adsorption experiments at three different temperatures at a constant *p*H of 7. The adsorption isotherms of (+)-catechin on Fe_3O_4/carbon and β-CD coated Fe_3O_4/carbon nanocomposite at three different temperatures are shown in Fig. 5(a) and Fig. 5(b). The adsorption intensity increases with decrease in temperature indicating that the adsorption process exothermic in nature. The temperature dependent adsorption affinity (q/C_e) was calculated from the slopes of individual isotherms in the linear region where all the isotherms could be extrapolated to the origin and these data were interpreted in terms Van't Hoff relation given by equation 6. The typical Van't Hoff plot for (+)-catechin adsorption on β-CD coated

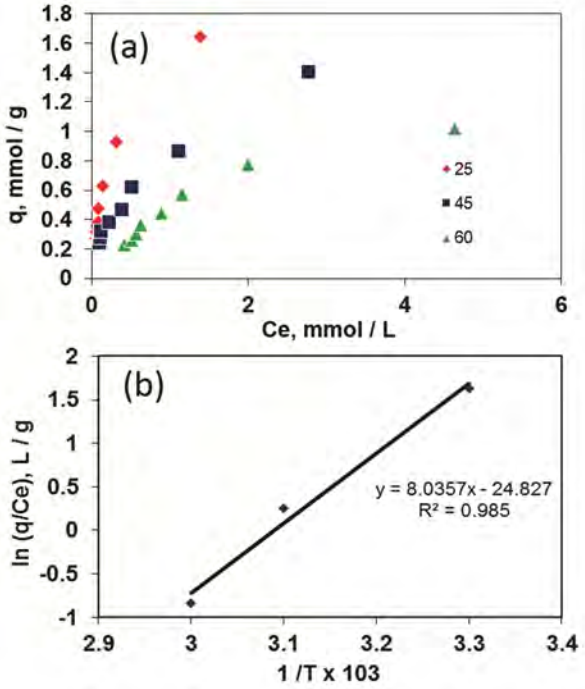

Fig. 5 — Adsorption of (+)-catechin on β-CD coated Fe_3O_4/carbon at different temperatures (a) and typical Van't Hoff plot for adsorption of (+) catechin on β-CD coated Fe_3O_4/carbon (b).

Fe_3O_4/carbon nanocomposite is shown in Fig. 5(b) and the estimated value of ΔH^0 is found to be -15.98 kcal / mol (R^2 =0.985).

The adsorbents which show highest affinity towards adsorbates, also shows the highest adsorption enthalpy which give an idea about the solute-sorbent binding interactions[36,37,40]. The adsorption of phenolic compounds exhibited identical behavior of high adsorption affinity corresponds to the adsorption enthalpy. Our experimental adsorption enthalpy for β-CD coated Fe_3O_4/carbon nanocomposite is comparable with the others reported in literature which corresponds to high adsorption affinity[36,37].

Adsorption kinetics

The kinetics of an adsorption process gives the equilibrium times and column breakthrough for design of adsorption system. The adsorption rate curves for (+)-catechin molecules on Fe_3O_4/carbon and β-CD coated Fe_3O_4/carbon nanocomposites are shown in Fig. 6(a).

The rate curves show a fast initial uptake followed by a relatively slow approach to equilibrium which follows the first order kinetics. This observation indicates in general that film diffusion controls the solute uptake data initially, and the particle diffusion controls the solute uptake in the later stage.

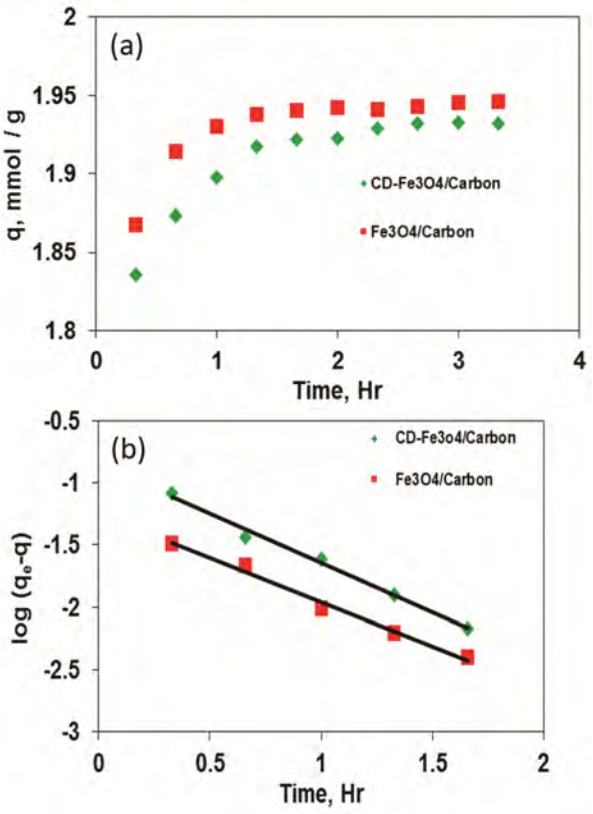

Fig. 6 — Adsorption rate curve for (+) catechin on β-CD coated Fe_3O_4/carbon (a) and Lagergren plot for tha adsorption of (+) catechin on β-CD coated Fe_3O_4/carbon and Fe_3O_4/carbon (b).

The fast adsorption is consistent with low external mass transfer at short times, whereas the slower adsorption at long time is consistent with a high intraparticle mass transfer resistance. Similar observations are reported in literature for the adsorption of tea catechins and antibiotics in polymeric resins and activated carbon[36,41]. The adsorption kinetics was faster for β-CD coated Fe_3O_4/carbon nanocomposites than for Fe_3O_4/carbon. For both the adsorbents the adsorption equilibrium was reached after 90 min of contact time. The kinetics for adsorption of (+)-catechin was examined with a first order rate expression, the so-called Lagergren equation [36]

$$\log (q_e\text{-}q) = \log q_e - (k_{ads} / 2.303)\, t, \qquad ...(7)$$

where, q_e and q are the amounts of (+)-catechin adsorbed (mmol/g) at equilibrium and any time (t) respectively, and $k_{ads}(s^{-1})$ is the adsorption rate constant. Fig. 6(b) shows a plot of $\log(qe - q)$ vs. *t*, which indicates first order kinetics representing the adsorption before attaining equilibrium. The value of the adsorption rate constant was found to be 1.442×10^{-5} s^{-1}, indicating a slow adsorption process.

The effect of external mass transfer on the adsorption kinetics can be analyzed by McKay equation valid for a linear isotherm and negligible intraparticle diffusion resistance[36]

$$\ln (C_t/C_0\text{-}1/1+mk) = \ln (mk/1+mk) - (1+mk/mk)\ \beta_1 S_s t \quad ...(8)$$

where, C_0 and C_t are the solute concentration initially and at any time (t), respectively, m (g l^{-1}) is the mass of adsorbent per litre of particle free slurry. The constant k is defined as $K_L x_m$ where K_L is the Langmuir constant ($lmmol^{-1}$) and x_m is the monolayer saturation (mmol g^{-1}), β_1 (cm s^{-1}) and S_s (cm^{-1}) are the mass transfer coefficients and particle surface area respectively.

S_s is given by the equation:

$$S_s = 6W / d_p\ \varphi_p (1- \varepsilon_p) \quad ...(9)$$

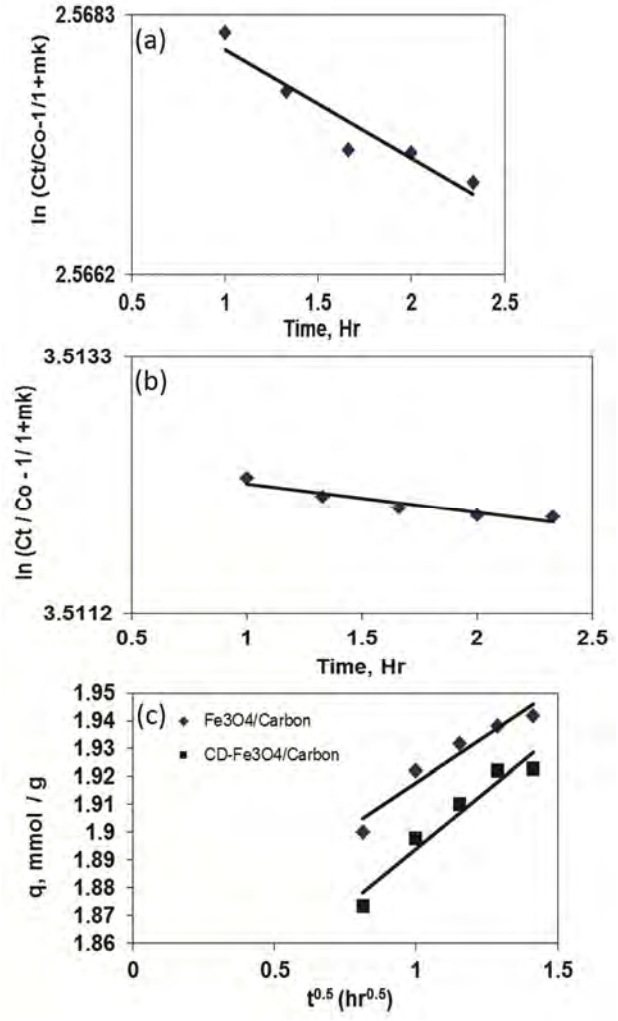

Fig. 7 — McKay plot for (+)-catechin adsorption on β-CD coated Fe_3O_4/carbon (a); McKay plot for (+)-catechin adsorption on Fe_3O_4/carbon (b) and intra- particular diffusion plot of (+)-catechin on activated carbon (c).

where, W is the weight, d_p is diameter, φ_p is the density and ε_p is the porosity (subscript 'p' refers to particle). Figure 7(a) and 7(b) shows the McKay plot in terms of ln [*Ct*/*C*0 −1/*mK*+1] vs. *t*. The role of external mass transfer in the adsorption process is indicated by the linearity of the plot. The mass transfer coefficient β_1 calculated from the slope and intercept of the plot was found to be 2.346×10^{-12} cm^{-1}. The deviation of the plot at the initial state of adsorption on the other hand**,** infers a different rate-controlling step.

The effect of intra-particle diffusion on the adsorption kinetics was examined from a graphical representation of qand the square root of time ($t^{0.5}$) as shown in Fig. 7(c). The near linearity of the plot for the adsorption of catechin onto β-CD coated Fe_3O_4/carbon nanocomposites infers the effect of intra-particle diffusion on the adsorption. However, as the plots are not passing through the origin, the pore diffusion alone may not be the rate-controlling step[36,42].

Conclusion

In this study, a carbon material from *Acacia Arabica* plant has been used for preparation of mesoporous Fe_3O_4/carbon nanocrystalline composite material and coated with β-CD as structure directing agents. The material shows smaller particle size around 20-35 nm and successively used as an adsorbent for separation of (+)-catechin from aqueous solutions. The adsorption equilibrium experimental data of (+)-catechin from aqueous solutions on Fe_3O_4/carbon and β-CD coated Fe_3O_4/carbon nanocomposite materials are interpreted from Langmuir and Freundlich isotherms. The adsorption process is *p*H dependent and β-CD coated Fe_3O_4/carbon nanocomposite provides the highest adsorption capacity because of its appropriate surface functional polarity. The equilibrium adsorption data exhibit better fit to Langmuir model for all the nano adsorbents studied in this work. The efficient adsorption along with the easy separation of the prepared catalyst exhibits that β-CD coated Fe_3O_4/carbon composite is a promising adsorbent for the removal of catechin from aqueous solutions.

Acknowledgement

Authors are thankful to Gauhati University, Guwahati for providing instrumental support.

References

1 Gramza A & Korczak J, *Trends Food Sci*, 16 (2005) 351.
2 Wiseman S A, Balentine D A & Frei B, *Crit Rev in Food Sci Nutr*, 37 (1997) 705.

3 Velayuthan P, Babu A & Liu D, *Curr Med Chem*, 15 (2008) 1840.
4 Spigno G & Faveri D D, *J Food Eng*, 93 (2009) 210.
5 Stalikas C D, *J Sep Sci*, 30 (2007) 3268.
6 Turkmen N, Velioglu Y S, Sari F & Polat G, *Molecules*, 12 (2007) 484.
7 Yoshida Y, Kiso M & Goto T, *Food Chem*, 67 (1999) 429.
8 Sharma V, Gulati A, Ravindranath S D & Kumar V, *J Food Comp Ana*, 18 (2005) 583.
9 Zarena A & Sankar K U, *J Super Fluids*, 49 (2009) 330.
10 Pelillo M, Toschi T G, Lercker G & Bonoli M, *Food Chem*, 81 (2003) 631.
11 Lozano C, Bujons J & Torres J L, *Sep Pur Tech*, 62 (2008) 317.
12 Wati R, Sampanvejsobha S & Punbusayakul N, *Agric Sci J*, 40 (2009) 47.
13 Manna M S, Bhatluri K K, Saha P K, Ghoshal A K, *Ind & Eng Chem Res*, 51 (2012) 15207.
14 Manna M S, Bhatluri K K, Saha P & Ghoshal A K, *J Memb Sci*, 447 (2013) 325.
15 Lozano C, Cascante M & Torres J L, *J Chromatogr A*, 973 (2002) 229.
16 Salas E, Duenas M, Schwarz M, Winterhalter P, Cheynier W & Fulcrand H, *J Agric Food Chem*, 53 (2005) 4536.
17 Murga R, Ruiz R, Beltran S & Cabezas J L, *J Agric Food Chem*, 48 (2000) 3408.
18 Lalaguna F, *J Chromatogr* A, 657 (1993) 445.
19 Zhangab H F & Shi Y P, *Analyst*, 137 (2012) 910.
20 Polshettiwar V, Luque R, Fihri A, Zhu H, Bouhrara M & Basset J M, *Chem Rev*, 111 (2011) 3036.
21 Yang J, Li J, Qiao J, Lian H & Chena H, *J Chroma A*, 1325 (2014) 8.
22 Chang P R, Zheng P, Liu B, Anderson D P, Yu J & Ma X, *J Hazard Mater*, 186 (2011) 2144.
23 Kaboudin B, Mostafalu R & Yokomatsu T, *Green Chem*, 15 (2013) 2266.
24 Badruddoz A Z M, Junwen L, Hidajat K & Uddin M S, *Colloids and Surf B: Biointe*, 92 (2012) 223.
25 Fan L, Luo C, Sun M, Qiu H & Li X, *Colloids Surf B*, 103 (2013) 601.
26 Yao Y, Miao S, Yu S, Ma L, Sun H & Wang S, *J Colloid Interface Sci*, 379 (2012) 20.
27 Fan L, Luo C, Li X, Lu F, Qiu H & Sun M, *J Hazard Mater*, 215–216 (2012) 272.
28 Lande M K & Navgire M E, *J Indust Engg Chem*, 18 (2012) 277.
29 Kang Y, Zhou L, Lib X & Yuan J, *J Mater Chem*, 21 (2011) 3704.
30 Cullity B, *Elements of X-Ray Diffraction, 2nd edn.* (Addison-Wesley, Massachusetts), 1978.
31 Navgire M E, Gogoi P, Mallesham B, A Rangaswamy, Reddy B M & Lande M K, *RSC Adv*, 6 (2016) 28679.
32 Huang J, Huang K, Liu S, Luo Q & Xu M, *J Colloid Interface Sci*, 315 (2007) 407.
33 Liu G, Yu H, Yan H, Shi Z & He B, *J Chromatogr A*, 952 (2002) 71.
34 Silva E M, Pompeu D R, Larondelle Y & Rogez H, *Sep Purif Technol*, 53 (2007) 274.
35 Ye J H, Jin J, Liang H L, Lu J L, Du Y Y, Zhang X Q & Liang Y R, *Bioresource Technol*, 100 (2009) 622.
36 Saikia M D & Dutta N N, *Colloid Surf A*, 280 (2006) 163.
37 Gogoi P, Saikia M D, Dutta N N & Rao P G, *Biochem Eng J*, 52 (2010) 144.
38 Otero M, Zabkova M & Rodrigues A E, *Sep & Purif Technol*, 45 (2005) 86.
39 Hall K R, Eagleton L C, Acrivos A & Vermeulen T, *Ind Eng Chem Fundam*, 5 (1966) 212.
40 Maity N, Payne G F & Chipchosky J L, *Ind Eng Chem Res*, 30 (1991) 2456.
41 Gogoi P, Dutta N N & Rao P G, *Ind J Chem Tech*, 17 (2010) 337.
42 Trivedi H C, Patel V M & Patel R D, *Eur Polym J*, 9 (1973) 525.